Assessing Earthquake Hazard Map Performance for Natural and Induced Seismicity in the Central and Eastern United States

by Edward M. Brooks, Seth Stein, Bruce D. Spencer, Leah Salditch, Mark D. Petersen, and Daniel E. McNamara

ABSTRACT

Seismicity in the central United States has dramatically increased since 2008, due in large part to the injection of wastewater produced by oil and gas extraction. In response to this phenomenon, the U.S. Geological Survey (USGS) created a one-year probabilistic hazard model and map for 2016 to portray the increased hazard posed to the central and eastern United States. Using the intensity of shaking reported to the "Did You Feel It?" (DYFI) system during 2016, we assessed the performance of this model using a metric that compared the fraction of sites at which the maximum shaking exceeded the mapped value to the fraction that had been expected. These fractions are similar for both the central and eastern United States as a whole, as well as for the region within this area with the highest amount of seismicity - Oklahoma and its surrounding area. We observe the greatest mismatch in northern Texas, with hazard overstated, presumably because lower oil and gas prices and regulatory action reduced the water injection volume relative to that of the previous year. We also assessed the model using a misfit metric that compares the spatial patterns of predicted and maximum observed shaking. This hazard map performs better by both metrics than other hazard maps we have studied. These results imply that such hazard maps can be valuable tools for policy makers and regulators in attempt to manage the seismic risks associated with unconventional oil and gas production.

INTRODUCTION

Since 2008, seismicity in the central United States has increased dramatically, largely due to the injection of wastewater produced by unconventional oil and gas extraction (Ellsworth, 2013; Keranen *et al.*, 2013, 2014; Kim, 2013; Hough, 2014; Rubinstein and Mahani, 2015; Weingarten *et al.*, 2015). This increased seismic activity poses a higher hazard than historically experienced areas that are generally unprepared for the resulting levels of shaking (Liu *et al.*, 2014; Ellsworth *et al.*, 2015).

The increased likelihood of damage necessitated reassessment of the seismic hazard in the area. Accordingly, the USGS produced a new seismic hazard map for the central and eastern United States (Petersen *et al.*, 2016a,b), which portrays the effects of both induced and natural seismicity (Fig. 1). The largest change to the most recent version of the map (the 2014 U.S. national seismic hazard map) that did not incorporate induced earthquake effects was the significantly increased hazard that was predicted in the area covering southern Kansas, Oklahoma, and northeast Texas (Petersen *et al.*, 2015). Induced seismicity was incorporated into the hazard map by defining zones where earthquakes do not appear natural, indicated by a noticeable increase in seismicity near injection wells, both spatially and temporally. Petersen *et al.* (2016a) define separate logic trees for seismicity inside and outside these zones, which differ largely in the parameters used to describe catalog duration, smoothing distance, maximum magnitude, and ground-motion models. Seismicity rates are inferred from injection rates of the prior year, which are assumed to be unchanged for 2016. The updated national map shows a probability of 5% to 12% of shaking at or above modified Mercalli intensity (MMI) VI in this area for the one-year time window in 2016, similar to the predicted hazard from natural seismicity in historically much more active regions such as California (Petersen *et al.*, 2016b).

The new model is a 1-yr forecast, showing the level of shaking that should have a 1% chance of exceedance at any point on the map during the year. The model used in making this map assumed that earthquake rates would remain relatively stationary and could be used to forecast shaking during 2016. This approach includes the effects of nontectonic earthquakes; this is in contrast to the 2014 model, which excluded nontectonic earthquakes.

Such one-year models are potentially valuable for policy makers and regulators dealing with the complex question of how to address the hazard due to induced earthquakes. To this end, we investigated how well the model forecasted the shaking

doi: 10.1785/0220170124

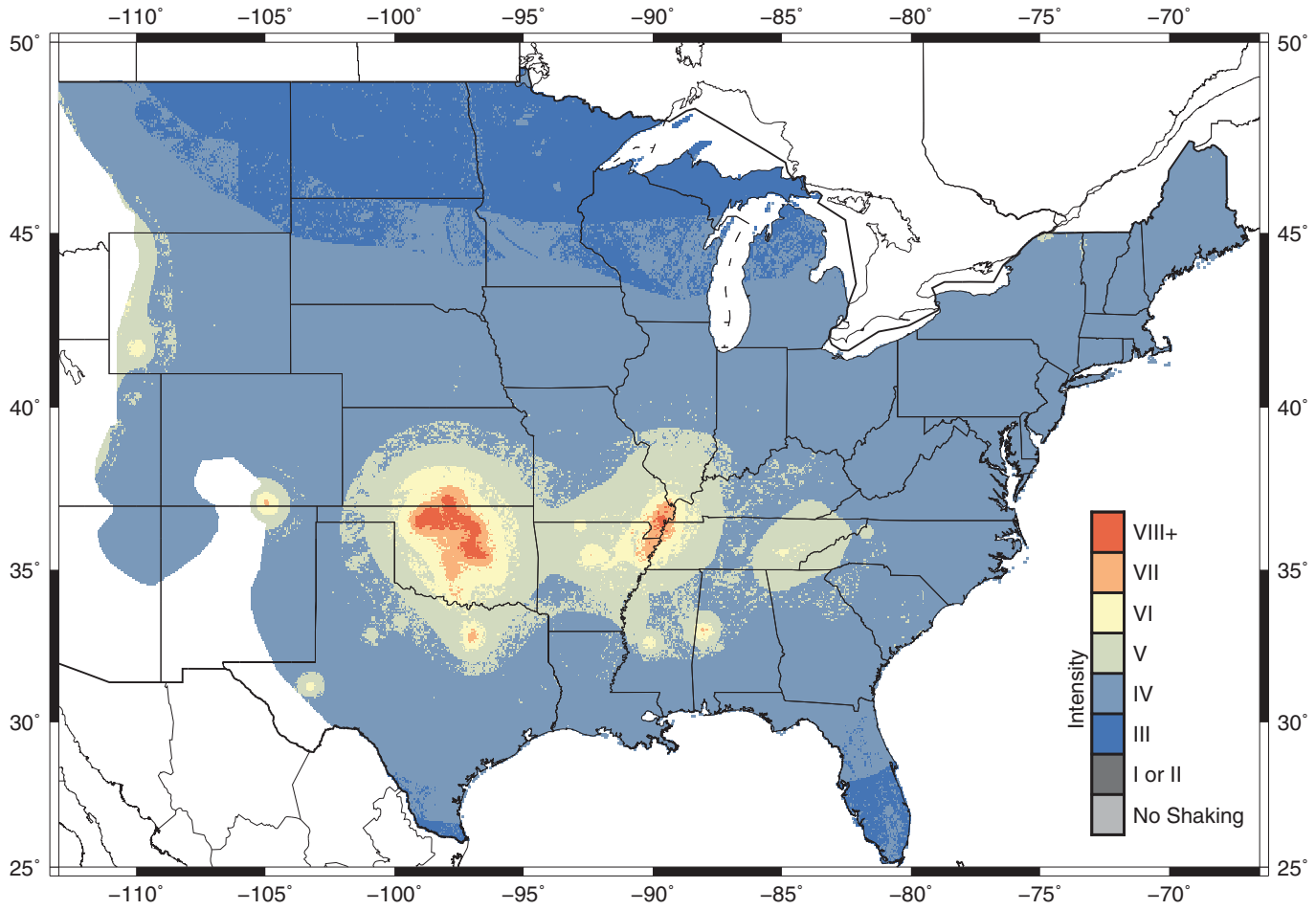

▲ **Figure 1.** 2016 One percent in one-year national seismic hazard map, showing the hazard for the central and eastern United States from induced and natural earthquakes (Petersen *et al.*, 2016a). The color version of this figure is available only in the electronic edition.

that actually occurred in 2016. We quantified the performance of the map using two metrics that summarized different aspects of the map's performance.

ASSESSING HAZARD MAP PERFORMANCE

Probabilistic seismic hazard models seek to predict a level of shaking that should be exceeded only with a certain probability over a given time window (Cornell, 1968; Field, 2010). At any point on the map, the probability p that shaking will exceed the value shown on a map during t years of observations with a T year return period is assumed to be described by an exponential distribution: $p = 1 - \exp(-t/T)$. For the one-year model, $t = 1$year, and $p = 0.01$ or 1%; with the given $T = 100$ yrs. Equivalently, on average, 1% of the sites should experience shaking greater than that shown on the map. This approach, introduced by Ward (1995) and used in many subsequent analyses (e.g., Albarello and D'Amico, 2008; Fujiwara *et al.*, 2009; Stirling and Gerstenberger, 2010; Nekrasova *et al.*, 2014; Tasan *et al.*, 2014; Mak and Schorlemmer, 2016a), considers many sites in order to ameliorate the rarity of large motions at any given site.

In this study, we assess the performance of earthquake hazard maps, using two metrics to numerically compare a map's predictions to records of shaking (Stein *et al.*, 2015). The first metric, the fractional exceedance metric $M0$, is described as follows:

$$M0(f, p) = |f - p|,$$

in which p is the predicted fraction of sites where the highest shaking during the study period is expected to exceed the modeled predictions, and f is the observed fraction of sites where this actually occurred. This metric, which is implicit in the probabilistic seismic hazard analysis (PSHA) methodology, is binary (above or below) and does not account for the size of the difference between predicted and observed shakings. We thus also use a second metric; this is $M1$, the squared misfit metric, which is described as follows:

$$M1(s, x) = \sum (x_i - s_i)^2 / N$$

in which the maximum observed shaking and predicted shaking (x_i and s_i) are compared during the study period at each of the sites $i = 1, ..., N$ (Stein *et al.*, 2015). For the purposes of

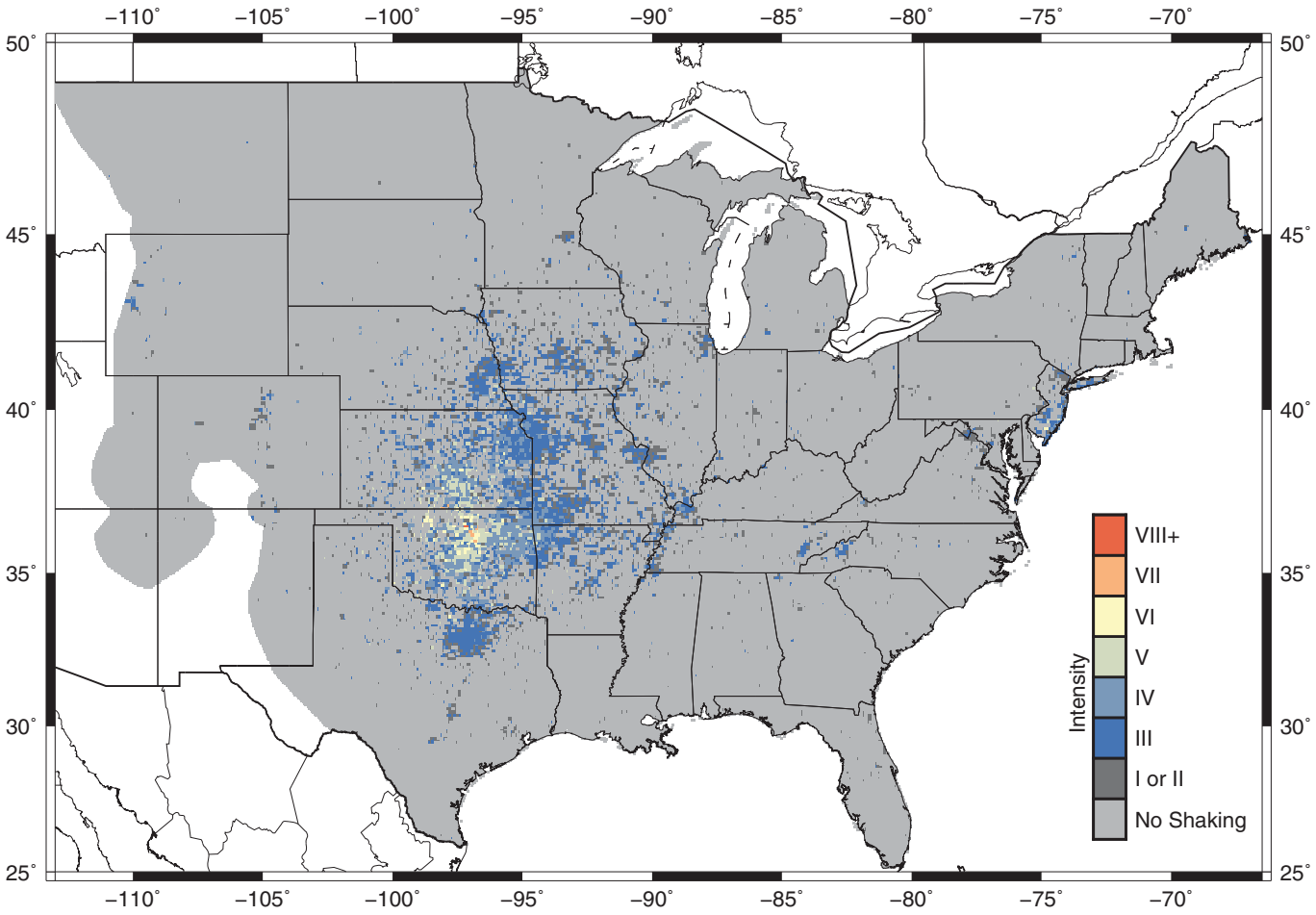

▲ **Figure 2.** Maximum reported shaking recorded from "Did You Feel It?" (DYFI) in 2016 for the central and eastern United States. The color version of this figure is available only in the electronic edition.

this study, the predicted shaking s_i is the level of shaking that has a 1% chance of exceedance throughout 2016.

For both metrics, a perfect match between prediction and observation would yield a score of 0. The two metrics characterize different aspects of map performance; hence, together they give a fuller picture of map performance than one measure could (Brooks *et al.*, 2016, 2017). $M0$ is sensitive to how well the map predicts average shaking levels. $M1$ is more sensitive to how well a map predicts spatial variations in shaking. Visually comparing maps of predicted and observed shakings amounts to using $M1$. Decomposition of $M0$ into systematic and random components of error is discussed in Stein *et al.* (2015), along with the attenuating effect of spatial correlation on the nominal sample size. The expected value of $M1$ is equal to the variance of the probability distribution of the maximum intensity plus $\sigma^2 + (\mu - r)^2$, with σ^2 as the variance, μ as the mean, and r as the $(100 - p)$th percentile of the probability distribution of maximum intensity over the time window of length T. Unfortunately, we have neither data for estimating the spatial correlation of the data and model, nor information about the probability distribution of the maximum intensity.

COMPARISON TO OBSERVED SHAKING

To assess the performance of the 2016 model, we need a record of shaking observed in 2016. The best and most extensive data available are from the "Did You Feel It?" (DYFI) database (Wald *et al.*, 1999; Atkinson and Wald, 2007). DYFI is an online tool that allows anyone who experiences ground motion to report it. Responses are compiled and geocoded by zip code to characterize the shaking distribution from an earthquake. After a year of data are collected, the USGS compiles maps of the annual maximum shaking at sites reported to the DYFI system, gridded at a 10 km resolution (Quitoriano *et al.*, 2017). Despite possible issues of quality and data completeness, DYFI is considerably more complete than available instrumental data and has proven to be one of the most thorough and robust datasets available (Wald *et al.*, 2012).

The 2016 maximum DYFI response map (Fig. 2) shows large areas of the central and eastern United States with no responses, with clusters of responses in the most seismically active regions. Absence of response can occur either because no shaking was felt, or because no one responded to DYFI after an earthquake, perhaps due to low population or earthquake

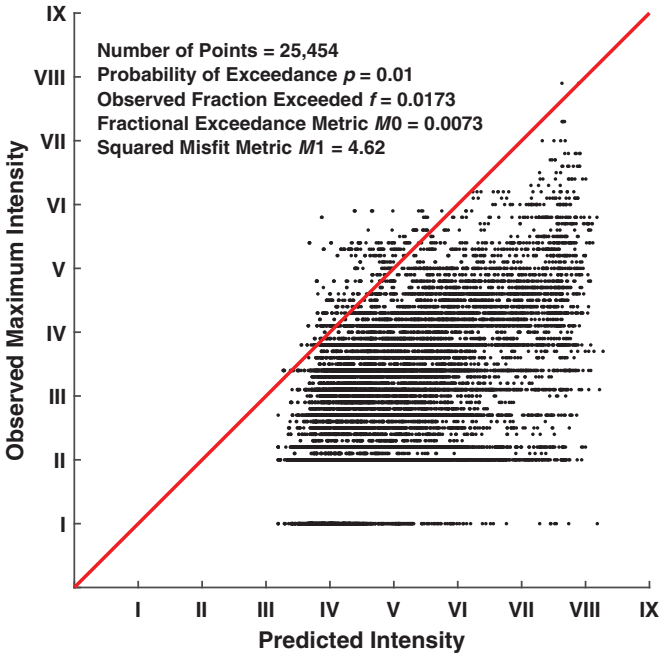

▲ **Figure 3.** Comparison plot of 2016 map predictions and 2016 DYFI observations for all points with a DYFI response in the central and eastern United States. The color version of this figure is available only in the electronic edition.

fatigue following numerous events (Mak and Schorlemmer, 2016b). The assumption that all regions without a response did not experience shaking is unrealistic, especially given the low populations in portions of the study area. Furthermore, such treatment would incorrectly imply that the map severely overpredicts shaking. Instead, we treat regions lacking responses as null or missing values and exclude them in evaluating the metrics.

Across the entire central and eastern United States, roughly 10% (25,454 out of 236,578 points) of the map exhibits a DYFI response. We use all the points, keeping in mind that spatial correlation among the shaking at these points vastly reduces the effective sample below the nominal 25,454. The comparison between the predicted and the observed maximum shakings is plotted in Figure 3. The fractional exceedance metric $M0$ compares the fraction of points f above the diagonal line (the region in which the largest observed shaking exceeds prediction) to the expected fraction p. About 1% of all sites should be above this line, and the actual fraction is 1.73%, leading to a fractional exceedance of $M0 = 0.0073$. The squared misfit metric $M1$ is 4.62, reflecting the visual similarity between the hazard map predictions and the map of maximum observed shaking (Figs. 1 and 2).

The difference between 1% and 1.73% site exceedances results from a few hundred more exceedances than expected. In order to see how large of a mismatch this is, we considered how much of an increase in predicted shaking would make $p = f = 0.01$ and thus $M0 = 0$. This would occur if the average predicted shaking were 0.24 MMI units, or 5% higher, than that predicted. This would decrease the number of exceedances observed to exactly that predicted.

THE GREATER OKLAHOMA AREA

When considering these results, it is important to note that the data are sparse on a national scale. We thus also examined the most seismically active portion of the mapped area. Figure 4 shows the predicted shaking and the maximum observed shaking for this greater Oklahoma area. Here, data completeness is improved relative to the entire region, with 45% (10,160 out of 22,560) of sites having DYFI responses.

Figure 5 shows the metrics for this smaller area. The fractional exceedance metric $M0 = 0.0069$ shows that the fraction of sites in this area experiencing higher than expected shaking is about the same as for the entire area $M0 = 0.0073$. The squared misfit metric increases slightly from $M1 = 4.62$ to 5.01.

The only notable difference between observation and prediction occurs for the Dallas area, where the map overpredicts the amount of shaking. Despite a maximum shaking of intensity VII, enough for moderate damage, that was forecasted, the highest shaking widely reported is of intensity III. This difference explains the increase in the squared misfit metric relative to the map as a whole, because a larger percentage of the local map is misfit; this portion covers roughly 15% of the greater Oklahoma region both in area and number of DYFI reports.

The mismatch in Dallas could be most easily explained in two different ways. The simplest is that the DYFI data reflect the actual shaking that the map overpredicted. Alternatively, perhaps fewer people in Dallas responded to DYFI, leading to underreporting of the maximum shaking. However, investigation into the DYFI data refutes the latter explanation. As shown in Figure 6, there appears to be a strong relationship between the number of reports that contribute to the maximum observed shaking and population, but not the intensity of the maximum shaking. The DYFI system seems to be well enough known to yield good reporting from a large population, even without intense shaking (Mak and Schorlemmer, 2016b).

It thus appears that the mismatch between observation and prediction in the Dallas region reflects a decrease in seismicity. The 2016 model assumed a constant level of human activity, meaning wastewater injection rates remaining unchanged. However, unconventional oil development is tied closely to economic factors (Campbell and Laherrère, 1998; Murray, 2016). Perhaps due to changing oil prices, or in response to seismicity assumed to be associated with wastewater injection, injection rates in northern Texas diminished in 2016 rather than staying stable (Hornbach *et al.*, 2016; Kuchment, 2017). As a result, the model overpredicted the shaking in 2016. A similar but smaller decrease in seismicity is also occurring in Oklahoma (Murray, 2016).

SUPPLEMENTING MISSING DATA

The fact that DYFI only has responses from about half of the greater Oklahoma area prompts the question of how the data set can be supplemented for a more thorough picture. Null

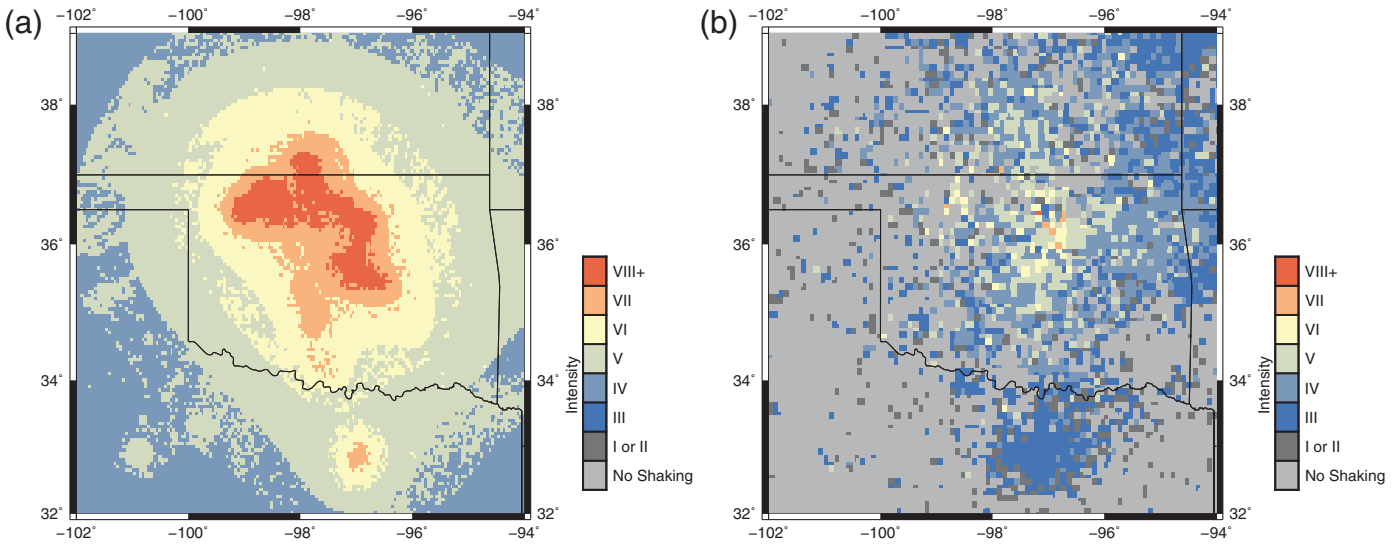

▲ **Figure 4.** (a) 2016 one-year seismic hazard model for induced and natural earthquakes for the greater Oklahoma region (Petersen *et al.*, 2016). (b) Maximum reported shaking recorded from DYFI in 2016 for this region. The color version of this figure is available only in the electronic edition.

responses do not necessarily imply that no shaking has occurred, and gaps between regions with reports of high shaking where reports of shaking are low or missing are likely to reflect a low population rather than a low amount of shaking. One approach is to set nonreporting regions to intensity I, which is "not felt" (Boatwright and Phillips, 2017). However, setting null points to intensity I is similar to setting them to 0 in that it also unfairly penalizes the map.

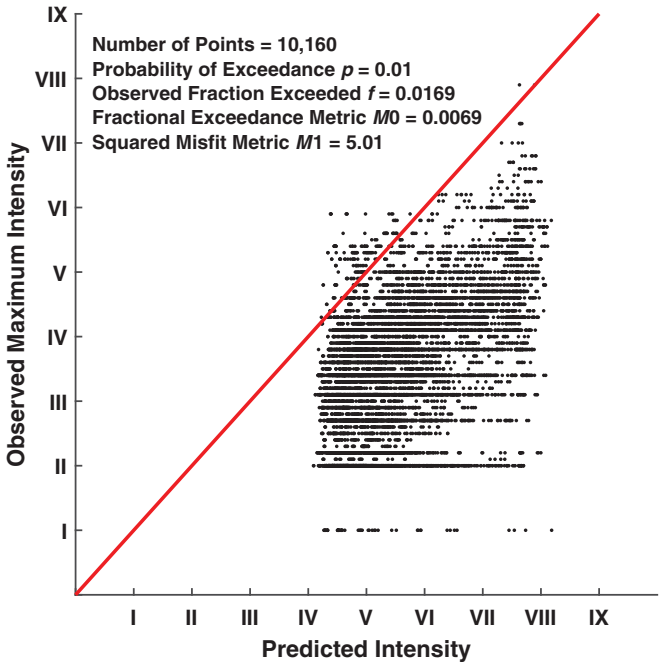

▲ **Figure 5.** Comparison of 2016 map predictions and DYFI observations for all points with a DYFI response in the greater Oklahoma region. The color version of this figure is available only in the electronic edition.

One alternative is to use models of expected shaking following known earthquakes to fill in sites without reported DYFI intensities. The USGS ShakeMap program predicts ground shaking following an earthquake, taking into account its magnitude, location, and geologic setting (Wald *et al.*, 2005). Although it is a model, as opposed to the direct observations provided by DYFI, ShakeMap provides reasonably accurate data augmentation in null regions and regions where the reported shaking is surprisingly low given their locations (Wald *et al.*, 2012).

In 2016, 21 earthquakes with magnitude 4.0 or greater occurred in the greater Oklahoma region. We selected a minimum magnitude of 4.0 in order to reduce the difficulty of assembling a dataset; this was done with the assumption that the distribution of earthquakes across the region was sufficiently spread out, such that smaller events would not produce higher shaking than from the larger events. Figure 7a shows the highest shaking modeled from the 21 earthquakes. ShakeMap predicts no exceedances relative to the hazard map, but the squared misfit is reasonably close to the original reported value. Hence, we conclude that there is no extreme bias toward high or low values in the ShakeMap predictions, and we treat the latter as minimum estimates of the maximum shaking at points without data.

Figure 7b shows the result of combining the ShakeMap predictions and DYFI data. In this combined dataset, almost 60% of the sites have a shaking value (13,427 sites out of 22,560). Figure 8 shows the metrics based on this combined dataset. Although the number of exceedances remains constant, the number of sites increases, decreasing the fraction of sites that exceed the predicted shaking. As a result, the fraction of sites exceeding the map predictions is 1.28%, yielding $M0 = 0.0028$. The squared misfit decreases to $M1 = 4.31$. These reductions suggest that the missing data, as well as

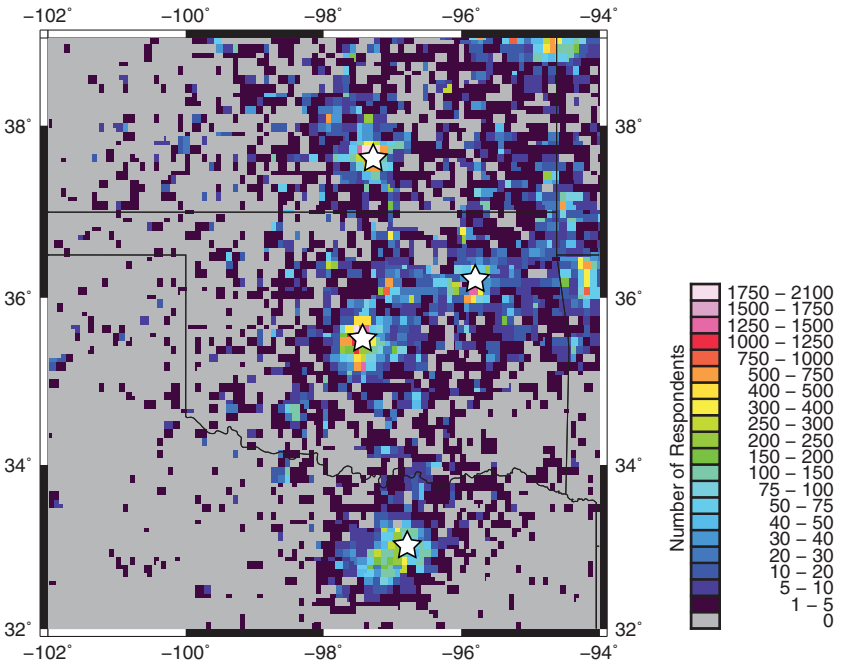

▲ **Figure 6.** Number of respondents who reported shaking when the maximum intensity DYFI event occurred. Stars denote major population centers. The color version of this figure is available only in the electronic edition.

anomalously low reports in areas of high shaking, made the map appear to perform more poorly than it actually did.

TRENDS IN DATA

In addition to calculating metrics, comparing the maximum observed and the predicted shakings (Figs. 3, 5, and 8) can highlight trends in the data and show how the map performance varies. The original DYFI data, in addition to maximum intensity and number of respondents, indicate the magnitude of the earthquake that caused the felt shaking. Figure 9a shows the predicted–observed plot for the greater Oklahoma region, with this magnitude data added to the original DYFI data. Although the database of shaking covers a wide range of magnitudes, the shaking reports are almost entirely dominated by the M_w 5.8 Pawnee earthquake, the largest recorded earthquake in the state of Oklahoma (Yeck *et al.*, 2017).

A few exceedances come from small events with M < 3.8. Of the 172 exceedances, 168 4 came from the Pawnee earthquake, and four came from other sources. The DYFI records only note the magnitude, number of respondents, and number of events that drove responses, so we do not know which specific small event prompted each of these exceedances.

Three earthquakes in Oklahoma in 2016 had M ≥ 5.0. Because each of these earthquakes had a different magnitude, the maximum DYFI reports associated with each magnitude can be given a known epicenter, and an epicentral distance from the site to each can be calculated. Figure 9b shows the predicted–observed plot as a function of distance for the sites where epicentral distance is known (96% of all DYFI observations). Both the predicted and the observed shaking decrease with distance, as expected. Exceedances arise primarily where the map predicts intensity IV–V shaking, and they come from a range of distances with no clear bias favoring one distance. A single exceedance for predicted intensity VIII appears to have occurred very close to the source event.

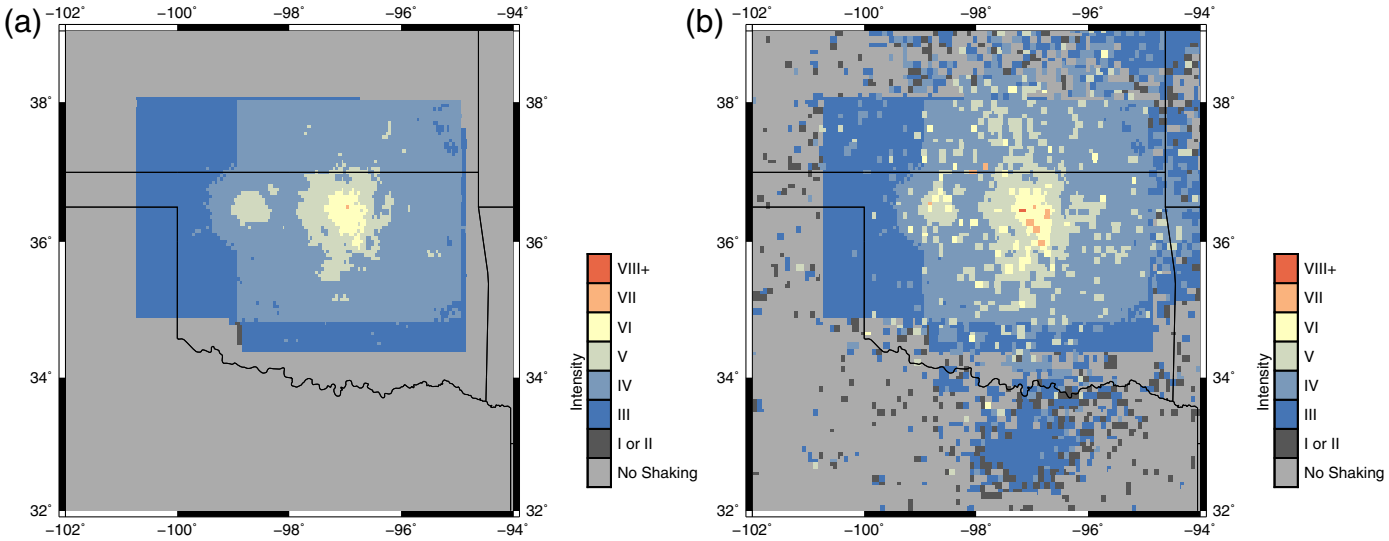

▲ **Figure 7.** (a) Maximum shaking predicted by ShakeMap for 21 earthquakes with magnitude greater than 4 in Oklahoma in 2016. (b) Result of combining ShakeMap predictions with existent DYFI data. The color version of this figure is available only in the electronic edition.

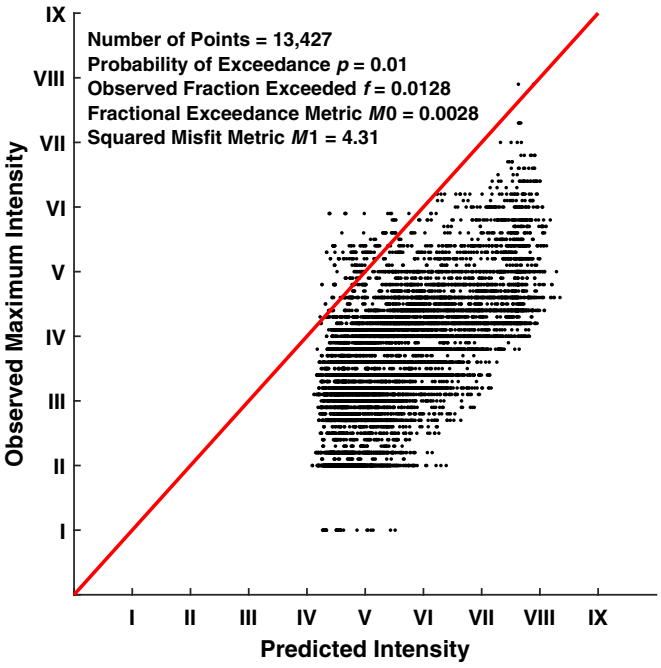

▲ **Figure 8.** Plot comparing 2016 map predictions to combined DYFI observations and ShakeMap predictions for the greater Oklahoma region. The color version of this figure is available only in the electronic edition.

Finally, we analyzed the spatial distribution of exceedances. We grouped sites in the greater Oklahoma region into a coarse 1.2° × 1.4° grid, such that the expected number of exceedances in each grid square was at least five. At this small scale, exceedances cluster (Fig. 10). Many regions have zero exceedances, leading to an incalculable fractional exceedance metric. The lack of exceedances in the south shows the overprediction in Dallas and north Texas. The high number in the northeast portion of the map shows where predictions were lower than the observed shaking.

CONCLUSIONS

The 2016 one-year national seismic hazard map for the central and eastern United States performed very well. It predicted the observed shaking well, as measured by both metrics. Because hazard map assessment is a relatively new enterprise, with only a few cases having been assessed thus far, there is currently no defined threshold for good scores on $M0$ and $M1$ metrics. This, along with the related question of how well a model could realistically be expected to describe observations, remains a question to be addressed in future work. However, the $M0$ fractional exceedance scores for the 2016 map are far lower than those for maps in our past studies (Stein *et al.*, 2015; Brooks *et al.*, 2016). In our view, $M0 = 0.0073$ on the national level and 0.0069 for the greater Oklahoma region

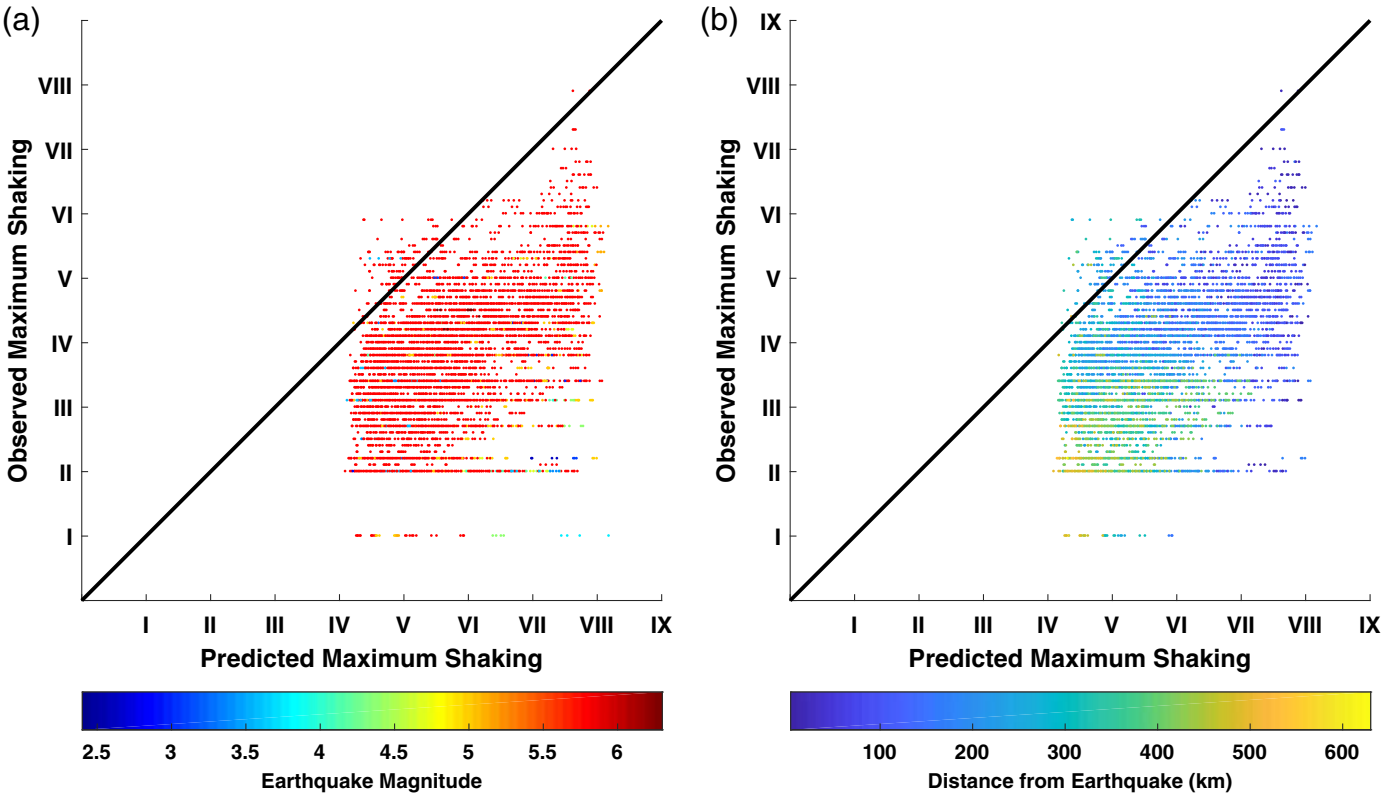

9 ▲ **Figure 9.** Plots comparing 2016 NSHM predictions to maximum DYFI observations for points with DYFI responses in the greater Oklahoma region, further broken down by (a) earthquake magnitude and (b) distance from source event (where that data are available). The color version of this figure is available only in the electronic edition.

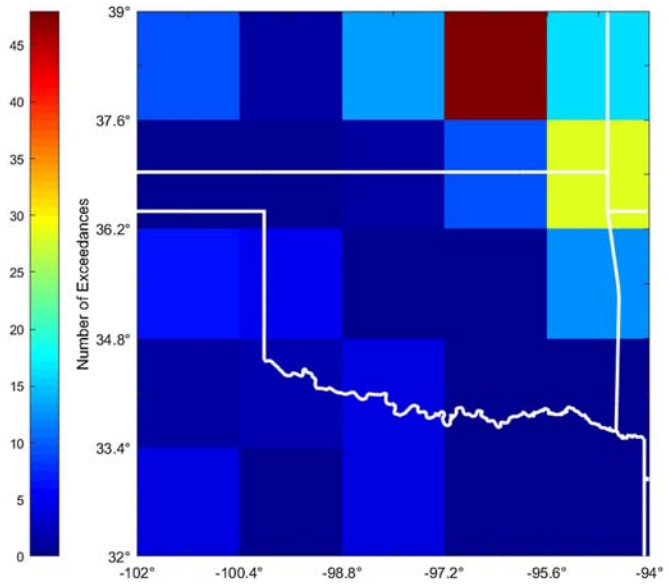

▲ **Figure 10.** Count of exceedances in site groups. Nine of twenty-five site groups have no exceedances, showing the limit of such a fine-scale breakdown. The color version of this figure is available only in the electronic edition.

indicate strong performance. The reduction to an even smaller $M0 = 0.0028$ when supplementing with ShakeMap data further reinforces the supposition that with additional information and a more thorough coverage of data, the hazard map succeeds in what is trying to do.

As noted, a 5% increase in the average predicted shaking for the national map would yield a perfect match between predicted and observed fractional exceedances. Such a small difference could easily occur by chance, related to which earthquakes occur in the short time period sampled (Vanneste *et al.*, 2017). The $M1$ squared misfit metric also demonstrates strong spatial (and hence visual) similarities between the predicted and the observed shaking maps. A map with a score of $M0 = 0$ may not be perfect, as there can easily be regions of overprediction balanced by areas of underprediction. However, when both metrics were combined, they suggested strong performance both in terms of fulfilling PSHA objectives and spatial accuracy. The model benefited from the fact that the 2016 seismicity rates across this region were generally similar to those observed during 2015 in Oklahoma.

The largest misfit occurred in northeastern Texas, where shaking was substantially overpredicted. This appears to reflect the limitations of the map's assumption that earthquake rates would remain relatively stationary, which would not be the case if water injection rates change due to regulatory or economic forces. Although this change highlights a limitation of the model, it indicates the value of making hazard maps for such short timescales in areas where induced seismicity is a major factor; economic and regulatory factors can change wastewater injection rates rapidly (Petersen *et al.*, 2017). This situation differs from natural seismicity hazard maps, where any time-dependent (earthquake cycle) effects occur on longer timescales.

Independently assessing successive one-year maps offers the prospect of improving the models used to generate them, in that the factors contributing to the map's performance (spatial variability, magnitude, ground-motion prediction model, etc.) can be evaluated. Similarly, as more is learned about the mechanisms of induced seismicity, this information can be included in the modeling. If successive models continue to perform well, or potentially even improve, they can be valuable tools for policy makers in managing the seismic risks associated with unconventional oil and gas productions.

DATA AND RESOURCES

The 2016 One-Year Seismic Hazard Model for the Central and Eastern United States from Induced and Natural Earthquakes was downloaded from https://www.sciencebase.gov/catalog/item/571a8e0ee4b071321fe22e7a. Maximum intensity "Did You Feel It?" (DYFI) data were provided by David Wald and Gregory Smoczyk and can be viewed at http://usgs.maps.arcgis.com/apps/webappviewer/index.html?id=931099 0e7ce84e3b8567109616b0944d. ShakeMap data were found on the U.S. Geological Survey (USGS) ShakeMap archives available at https://earthquake.usgs.gov/data/shakemap/ (Quitoriano *et al.*, 2017).

ACKNOWLEDGMENTS

The authors thank David Wald, Ken Rukstales, and Gregory Smoczyk for their help acquiring and using the "Did You Feel It?" (DYFI) datasets. The authors also thank two anonymous reviewers for helpful comments. Brooks thanks the Northwestern Institute for Policy Research for funding his research.

REFERENCES

Albarello, D., and V. D'Amico (2008). Testing probabilistic seismic hazard estimates by comparison with observations: An example in Italy, *Geophys. J. Int.* **175,** no. 3, 1088–1094.

Atkinson, G. M., and D. J. Wald (2007). "Did You Feel It?" intensity data: A surprisingly good measure of earthquake ground motion, *Seismol. Res. Lett.* **78,** no. 3, 362–368.

Boatwright, J., and E. Phillips (2017). Exploiting the demographics of "Did You Feel It?" responses to estimate the felt area of moderate earthquakes in California, *Seismol. Res. Lett.* **88,** no. 2A, 335–341.

Brooks, E. M., S. Stein, and B. D. Spencer (2016). Comparing the performance of Japan's earthquake hazard maps to uniform and randomized maps, *Seismol. Res. Lett.* **87,** no. 1, 90–102.

Brooks, E. M., S. Stein, and B. D. Spencer (2017). Investigating the effects of smoothing on the performance of earthquake hazard maps, *Int. J. Earthq. Impact Eng.* (in press).

Campbell, C. J., and J. H. Laherrère (1998). The end of cheap oil, *Sci. Am.* **278,** no. 3, 78–83.

Cornell, C. A. (1968). Engineering seismic risk analysis, *Bull. Seismol. Soc. Am.* **58,** no. 5, 1583–1606.

Ellsworth, W. L. (2013). Injection-induced earthquakes, *Science* **341,** no. 6142, 1225942.

Ellsworth, W. L., A. L. Llenos, A. F. McGarr, A. J. Michael, J. L. Rubinstein, C. S. Mueller, M. D. Petersen, and E. Calais (2015). Increasing seismicity in the US midcontinent: Implications for earthquake hazard, *The Leading Edge* **34,** no. 6, 618–626.

Field, E. H. (2010). *Probabilistic Seismic Hazard Analysis: A Primer*, available at http://www.opensha.org/ (last accessed May 2017).

Fujiwara, H., N. Morikawa, Y. Ishikawa, T. Okumura, J. I. Miyakoshi, N. Nojima, and Y. Fukushima (2009). Statistical comparison of national probabilistic seismic hazard maps and frequency of recorded JMA seismic intensities from the K-NET strong-motion observation network in Japan during 1997–2006, *Seismol. Res. Lett.* **80,** no. 3, 458–464.

Hornbach, M. J., M. Jones, M. Scales, H. R. DeShon, M. B. Magnani, C. Frohlich, B. Stump, C. Hayward, and M. Layton (2016). Ellenburger wastewater injection and seismicity in North Texas, *Phys. Earth Planet. In.* **261,** 54–68.

Hough, S. E. (2014). Shaking from injection-induced earthquakes in the central and eastern United States, *Bull. Seismol. Soc. Am.* **104,** no. 5, 2619–2626.

Keranen, K. M., H. M. Savage, G. A. Abers, and E. S. Cochran (2013). Potentially induced earthquakes in Oklahoma, USA: Links between wastewater injection and the 2011 M_w 5.7 earthquake sequence, *Geology* **41,** no. 6, 699–702.

Keranen, K. M., M. Weingarten, G. A. Abers, B. A. Bekins, and S. Ge (2014). Sharp increase in central Oklahoma seismicity since 2008 induced by massive wastewater injection, *Science* **345,** no. 6195, 448–451.

Kim, W. Y. (2013). Induced seismicity associated with fluid injection into a deep well in Youngstown, Ohio, *J. Geophys. Res.* **118,** no. 7, 3506–3518.

Kuchment, A. (2017). Are earthquakes gone from our area for good?, *Dallas News*, available at https://www.dallasnews.com/business/energy/2017/03/01/earthquakes-gone-area-good-scientists-try-solve-mystery (last accessed May 2017).

Liu, M., G. Luo, H. Wang, and S. Stein (2014). Long aftershock sequences in North China and Central US: Implications for hazard assessment in mid-continents, *Earthq. Sci.* **27,** no. 1, 27–35.

Mak, S., and D. Schorlemmer (2016a). A comparison between the forecast by the United States National Seismic Hazard Maps with recent ground-motion records, *Bull. Seismol. Soc. Am.* **106,** no. 4, 1817–1831.

Mak, S., and D. Schorlemmer (2016b). What makes people respond to "Did You Feel It?", *Seismol. Res. Lett.* **87,** no. 1, 119–131.

Murray, K. E. (2016). Seismic moment versus water: A study of market forces, *Geol. Soc. Am. Abstr. Progr.* **48,** no. 7, Paper 95-11.

Nekrasova, A., V. Kossobokov, A. Peresan, and A. Magrin (2014). The comparison of the NDSHA, PSHA seismic hazard maps and real seismicity for the Italian territory, *Nat. Hazards* **70,** no. 1, 629–641.

Petersen, M. D., M. P. Moschetti, P. M. Powers, C. S. Mueller, K. M. Haller, A. D. Frankel, Y. Zeng, S. Rezaeian, S. C. Harmsen, O. S. Boyd, *et al.* (2015). The 2014 United States national seismic hazard model, *Earthq. Spectra* **31,** no. S1, S1–S30.

Petersen, M. D., C. S. Mueller, M. P. Moschetti, S. M. Hoover, A. L. Llenos, W. L. Ellsworth, A. J. Michael, J. L. Rubinstein, A. F. McGarr, and K. S. Rukstales (2016a). *2016 One-Year Seismic Hazard Forecast for the Central and Eastern United States from Induced and Natural Earthquakes*, Number 2016-1035, U.S. Geological Survey.

Petersen, M. D., C. S. Mueller, M. P. Moschetti, S. M. Hoover, A. L. Llenos, W. L. Ellsworth, A. J. Michael, J. L. Rubinstein, A. F. McGarr, and K. S. Rukstales (2016b). Seismic hazard forecast for 2016 including induced and natural earthquakes in the central and eastern United States, *Seismol. Res. Lett.* **87,** 1327–1341.

Petersen, M. D., C. S. Mueller, M. P. Moschetti, S. M. Hoover, A. M. Shumway, D. E. McNamara, R. A. Williams, A. L. Llenos, W. L. Ellsworth, A. J. Michael, *et al.* (2017). 2017 One-Year Seismic-Hazard Forecast for the Central and Eastern United States from Induced and Natural Earthquakes, *Seismol. Res. Lett.* **88,** no. 3, 772–783.

Quitoriano, V., E. M. Thompson, G. M. Smoczyk, and D. J. Wald (2017). Access to "Did You Feel It?" data for induced earthquake studies, paper presented in the *2017 Seismological Society of America Annual Conference*, Denver, Colorado, 20 April 2017.

Rubinstein, J. L., and A. B. Mahani (2015). Myths and facts on wastewater injection, hydraulic fracturing, enhanced oil recovery, and induced seismicity, *Seismol. Res. Lett.* **86,** no. 4, 1060–1067.

Stein, S., B. D. Spencer, and E. M. Brooks (2015). Metrics for assessing earthquake-hazard map performance, *Bull. Seismol. Soc. Am.* **105,** no. 4, 2160–2173.

Stirling, M., and M. Gerstenberger (2010). Ground motion-based testing of seismic hazard models in New Zealand, *Bull. Seismol. Soc. Am.* **100,** no. 4, 1407–1414.

Tasan, H., C. Beauval, A. Helmstetter, A. Sandikkaya, and P. Guéguen (2014). Testing probabilistic seismic hazard estimates against accelerometric data in two countries: France and Turkey, *Geophys. J. Int.* **198,** no. 3, 1554–1571.

Vanneste, K., S. Stein, T. Camelbeeck, and B. Vleminckx (2017). Insights into earthquake hazard map performance from shaking history simulations, *Sci. Rep.* (in review).

Wald, D. J., V. Quitoriano, L. A. Dengler, and J. W. Dewey (1999). Utilization of the Internet for rapid community intensity maps, *Seismol. Res. Lett.* **70,** no. 6, 680–697.

Wald, D. J., V. Quitoriano, C. B. Worden, M. Hopper, and J. W. Dewey (2012). USGS "Did You Feel It?" Internet-based macroseismic intensity maps, *Ann. Geophys.* **54,** no. 6, doi: 10.4401/ag-5354.

Wald, D. J., B. C. Worden, V. Quitoriano, and K. L. Pankow (2005). *ShakeMap Manual: Technical Manual, User's Guide, and Software Guide*, Number 12–A1.

Ward, S. N. (1995). Area-based tests of long-term seismic hazard predictions, *Bull. Seismol. Soc. Am.* **85,** no. 5, 1285–1298.

Weingarten, M., S. Ge, J. W. Godt, B. A. Bekins, and J. L. Rubinstein (2015). High-rate injection is associated with the increase in US mid-continent seismicity, *Science* **348,** no. 6241, 1336–1340.

Yeck, W. L., G. P. Hayes, D. E. McNamara, J. L. Rubinstein, W. D. Barnhart, P. S. Earle, and H. M. Benz (2017). Oklahoma experiences largest earthquake during ongoing regional wastewater injection hazard mitigation efforts, *Geophys. Res. Lett.* **44,** no. 2, 711–717.

***Edward M. Brooks*[1]**
***Seth Stein*[1]**
Leah Salditch
Department of Earth and Planetary Sciences
Northwestern University
2145 Sheridan Road
Evanston, Illinois 60208 U.S.A
eddie@earth.northwestern.edu

***Bruce D. Spencer*[1]**
Department of Statistics
Northwestern University
2006 Sheridan Road
Evanston, Illinois 60208 U.S.A.

Mark D. Petersen
Daniel E. McNamara
U.S. Geological Survey
MS 966, Box 25046
Denver, Colorado 80225 U.S.A.

[1] Also at Institute for Policy Research, Northwestern University, Evanston, Illinois U.S.A.

QUERIES

1. AU: You have provided two affiliations for the first three authors. SSA only allows one primary affiliation, and the other affiliations are set as an author footnote. Please indicate which one should be treated as the primary affiliation.
2. AU: Please verify the affiliation data at the end of your article. Please clarify if the USGS address is "Denver, Colorado" or "Golden, Colorado".
3. AU: Please provide complete postal service address for this author footnote if available.
4. AU: Please indicate if the roman capital M throughout the article should be changed to (1) bold **M** or (2) M_w (italic "M" and subscript roman "w").
5. AU: Please provide the month and year when you last accessed the websites mentioned in Data and Resources for your article.
6. AU: For Brooks *et al.* (in press): SSA cannot include unpublished manuscripts in the References section. Please provide an update on the publication status of this article. At minimum, we need to have volume and doi numbers for an entry in the References to have "in press" status. If that is not available, then the article may be cited as an unpublished manuscript and details included in the Data and Resources section (if desired). Citations would be changed to a format such as "... from E. M. Brooks, S. Stein, and B. D. Spencer (unpublished manuscript, 2017; see Data and Resources)."
7. AU: For Vanneste *et al.* (in review): SSA cannot include unpublished manuscripts in the References section. Please provide an update on the publication status of this article. At minimum, we need to have volume and doi numbers for an entry in the References to have "in press" status. If that is not available, then the article may be cited as an unpublished manuscript and details included in the Data and Resources section (if desired). Citations would be changed to a format such as "... from K. Vanneste, S. Stein, T. Camelbeeck, and B. Vleminckx (unpublished manuscript, 2017; see Data and Resources)."
8. AU: There are two "Petersen *et al.*, (2016)" references in the Reference section (denoted as 2016a and 2016b). Please specify which is being cited here.
9. AU: Please provide a definition of "NSHM"; it will be included before the abbreviation.